Berhan International Research Journal of Science and Humanities (BIRJSH), 2024, 8(1), 30-48

Journal homepage: www.journals.dbu.et *ISSN: 2414-2794 eISSN: 3006-578X*

Near Real Time Crop Health Status Monitoring and Mapping using Sentinel Satellite Image in Menjar Shenkora District, Ethiopia

Awlachew Dejen[1], Ayele Behailu[1], Estifanos Lemma[2]*

[1]Department of Geography and Environmental Studies, Debre Berhan University, Debre Berhan, Ethiopia

[2]Department of Natural Resource Management, Debre Berhan University, Debre Berhan, Ethiopia

DOI: https://doi.org/10.61593/DBU.BIRJSH.01.08.02

Abstract

Agricultural monitoring systems must provide timely and standardized information on crop production, status, and yield, from sub-regional to national scales. Accurate monitoring and mapping of vegetation condition and health are vital for managing crops, assessing damage, and predicting yields. Crop health monitoring is one of the important items for tracking the general health status of any crop. In this regard, remote sensing and GIS play a crucial role for monitoring crop health, providing current information that traditional methods like field surveys and sampling questionnaires struggle to obtain. Effective cropland mapping techniques are essential for regular crop monitoring. This type of monitoring demands frequents continuous data with high time and space resolution. Near real-time crop monitoring uses technologies like the Sentinel-2 satellite mission, offering a consistent 5-day revisit cycle and freely accessible data. This opens new doors for delivering timely updates and monitoring parcel-based crop health and conditions in real-time. Therefore, this study used satellite images, Global Positioning System (GPS) collected data, and parcel-based socioeconomic data. GPS and socioeconomic data were employed to validate the satellite-based near real-time crop monitoring results. Vegetation Condition Index (VCI) and the Normalized Difference Vegetation Index (NDVI) were used to evaluate crop health at different stages of the growing season and to generate time series data for crop phenology respectively. NDVI time series data was used to generate crop phenology information for four main crops: Teff, wheat, onion, and sorghum. The crop type maps for these crops at the study sites were validated with an overall accuracy of 79.26% and a Kappa value of 0.737. Additionally, the results from the current research and the field-collected data were consistent in providing information about the onset, greening, maturity, and senescence dates of each crop. These findings highlight the effectiveness of the satellite-based system for real-time agricultural crop monitoring using Sentinel-2 observations across various sites and time frames. Moreover, it helps to fill the gaps of traditional crop monitoring methods with those based on satellite technology. This system is particularly valuable for early warning purpose in areas like the current study site, where conventional crop monitoring methods and inputs are limited.

Keywords: Crop mapping; GIS; Minjar Shenkora; near real time; Sentinel images; Ethiopia

*Corresponding author email: estfnlm@gmail.com

Article information: Received 05 May 2023; Revised on 21 September 2024; Accepted on 11 November 2024

Introduction

Agricultural monitoring systems must provide prompt and standardized data on crop production, status, and yield, extending from sub-regional and national levels. Estimates need to be provided as early in the growing season as possible and regularly updated until harvest (Matteo et al., 2022). With the provided information, stakeholders can make early decisions and pinpoint areas with significant variations in production and productivity (Atzberger, 2013). Accurate monitoring and mapping of vegetation condition and health are are vital for managing crops, assessing damage, and predicting yields (Zhang et al., 2019). Green vegetation can be monitored by observing its spectral reflectance characteristics (Tucker et al., 1979). Nowadays, satellite sensors regularly supply diverse data across multiple spectral ranges. This aids in monitoring crops for numerous agricultural and ecological purposes, including preventing disease and pest outbreaks, estimating crop yields, managing water resources, and optimizing fertilizer use (Mass, 1988; Hatfield et al., 1993; Duchemin et al., 2015; Diacono et al., 2013; Bouchet, 2016).

Remote sensing time series data are essential for analyzing and comprehending changes in land cover. This data enables tracking crop seasonality across various time frames, with communities typically following yearly growth patterns. Yearly variations in phonological markers, like the start of greenness and the duration of the growing season, are influenced by short-term climate changes (Bradley et al., 2007). Detecting disturbances in real-time is essential for identifying anomalies, issuing timely alerts, and minimizing negative effects on population, infrastructure and natural resources (Verbesselt et al., 2012). For many years, satellite remote sensing has been highlighted as a crucial data source for operating agricultural monitoring. Due to their daily revisit rates, global coverage, extensive archives, and freely accessibility, optical instruments with coarse to medium resolution on satellites like SPOT-Vegetation, AVHRR (Advanced Very Haigh-Resolution Radiometric) and MODIS (Moderate Resolution Imaging Spectrometer) are vital for near real-time and frequent crop monitoring (Defourny, et al., 2019).

In Ethiopia, about 83.9% of the population resides in rural areas, with agriculture being their main source of livelihood. Since 2010, agriculture has been the most important sector after services, employing

80% of the workforce, accounting for 70% of foreign exchange earnings, and contributing 42.7% to the GDP (CSA, 2013; NBE, 2013). These statistics highlight the crucial role of agriculture in Ethiopia's employment, GDP contribution, and exports. Ethiopia has a substantial agricultural potential due to its extensive fertile land, adequate rainfall, diverse climate, and plentiful labor force. However, the agricultural sector remains underdeveloped despite these advantages. Since the early 1970s, progress has been hindered by recurring droughts, limited technology, inadequate infrastructure, and a fragile economic foundation marked by low productivity, as well as overpopulation. For example, between 1980 and 1987, the World Bank noted that agricultural output decreased by 2.1% each year, whereas the population increased by 2.4% annually. This led to a famine from 1984 to 1986, resulting in nearly 1 million deaths (Wubne, et al. 1991). Hence, addressing famine and improving crop productivity are critical issues.

Remote sensing technology provides wide satellite data, which is highly effective for monitoring vegetation dynamics because of its extensive coverage and frequent temporal sampling (Atzberger, 2013). Monitoring crop health is crucial for assessing the overall condition of crops. Utilizing Geographic Information System (GIS) and remote sensing technologies are beneficial for crop health monitoring, as they provide up-to-date information that is challenging to gather through traditional methods like field surveys and questionnaires (Prathumchai, 2001). In Ethiopia, conventional methods for monitoring crops rely significantly on climatological data, which is both time-consuming and labor-intensive to gather. Additionally, disseminating this data poses significant challenges. As a result, millions of lives might be affected before decision-makers receive the essential information. The data produced by these conventional methods is often too uncertain to support preventive measures, making the generation of reliable and timely information for decision-makers critically important (Getachew et al., 2011).

Effective crop monitoring requires consistent and frequent data collection at regular intervals, with high spatial and temporal resolution. Numerous satellite imageries including AVHRR, MODIS and SPOT Vegetation provide data were used at different resolutions, ranging from below 1 meter to 1000 meters. The information which is obtained from such satellite image is very coarse for parcel level crop monitoring and mapping. Previously, no specific crop health monitoring was conducted at the study site using recently available high-resolution satellite imagery. Hence, this research attempted to address that gap by utilizing newly accessible satellite data sources to monitor crop health. Due to this, the present study employed time series data from Sentinel 2 satellite imagery, benefiting from its improved spatial resolution (10 meter for optical bands). Thus, the primary purpose of this research was to monitor and map crop health status in the Menjar Shenkora district of North Shewa Zone, Ethiopia. The specific objectives included: (i) analyzing crop phenology for the main crop types in the study site; (ii) monitoring the health status of these major crops; and (iii) producing updated crop health information.

Materials and Methods

Location of the study area

Minjar Shenkora district, the study area, is situated in the North Shewa Zone of Ethiopia's Amhara Region. It is the southernmost Woreda of North Shewa zone and its extent is in between 8^0 41' 42''N - 9^0 6'39''N to 39^0 13'0''E- $39^0$44'33'' E (Fig. 1). In this district there are about 29 kebeles (smallest administration unit) with a total area of 1511km^2. It is bordered on the east, south and west by the Oromia Region, on the northwest by Hageremariamna Kesem district, and on the northeast by Berehet district.

Data type and data sources

The data for this research was gathered from various sources. Table 1 details the data types and their sources.

Sentinel 2 Satellite image

To monitor land surfaces and agriculture, the European Copernicus program developed the Sentinel-2 satellite constellation with its Multi-Spectral Instrument (MSI).

This instrument measures a wide range of solar reflectance from visible to shortwave infrared bands (Gascon et al., 2017). The bands include three red-edge bands and two shortwave infrared bands at 20m resolution, providing crucial vegetation data, three narrow bands for cloud screening and atmospheric correction at 60m resolution, and standard blue, green, and infrared bands at 10m resolution (Gascon et al., 2017).

Since late 2015, the Sentinel-2A satellite has provided a 10-day revisit time over Europe and Africa, and a 20-day revisit time elsewhere. Additionally, since February 2018, Sentinel-2B has guaranteed a 5-day revisit time over all landmasses. Sentinel satellite images also offer a spatial resolution of 10 meters for blue, green, and near-infrared bands, with a high temporal resolution of approximately every 5 days. Due to these advantages, Sentinel satellite images were utilized for this study.

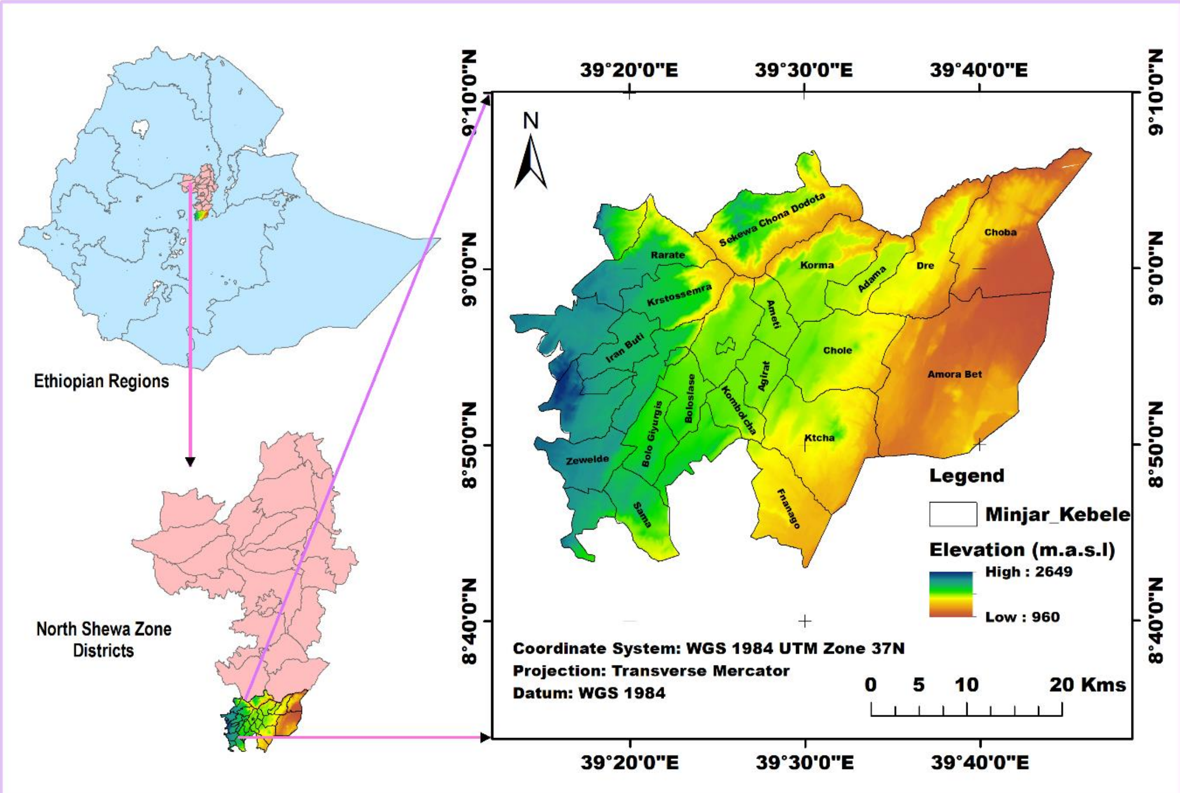

Figure 1. Location map of the study site

Table 1: Data types and their sources

SN	Data type	Source	Purpose
1	Sentinel-2B satellite image	https://scihub.copernicus.eu/	To acquire optical data with 10m spatial resolution
2	Parcel data	North Shewa Rural land Administration Office	To generate parcel level geo-information
3	Ground Control Point (GCP)	Field measurement	Validation
4	Phenology information	Key informant interview	To collect information about the growing season and phonological stages of crops

Parcel data

The parcel data served as a mask when calculating the normalized difference vegetation index (NDVI). This research focused solely on crop health status, necessitating the exclusion of other land uses and land covers.

Normalized difference vegetation index

The reflection and absorption levels in the near-infrared spectrum are crucial indicators of vegetation health. To assess the vegetation health, different indexes were utilized. Among them, NDVI is the most commonly utilized index by various institutions and organizations, including the United States Famine Early Warning System Network (FEWS-NET), the United Nations Food and Agricultural Organization (FAO), and the Monitoring Agricultural Resources (MARS) unit at the Joint Research Centre (JRC) (Rojas et al., 2008). This index serves as an early warning tool for potential food production issues in African countries. It is calculated by dividing the difference between the near infrared (NIR) and the red bands to the sum of these two bands (Rouse et al., 1984).

$$\mathrm{NDVI} = \frac{\mathrm{NIR}-\mathrm{RED}}{\mathrm{NIR}+\mathrm{RED}} \quad \text{(eq.1)}$$

Where, NIR means near-infrared reflectance and RED represents red reflectance. In the existing study, Sentinel-2 images were used to calculate NDVI. Particularly band 8 was used for NIR and band 4 was used for RED. NDVI values range from +1 to -1, with higher positive values indicating dense, healthy vegetation, while lower or negative values signify inconsequential or unhealthy vegetation cover.

NDVI anomaly

The NDVI anomaly measures the difference between the current value and the long-term average. The resulted positive anomaly indicates better vegetation conditions than the average vegetation conditions, while a negative anomaly value suggests lower vegetation condition than the average conditions. This method is widely used to detect and map drought and vegetation health by comparing the current NDVI to its long-term mean for a specific pixel or region at s specific period (Anyamba and Tucker, 2012). Hence, to calculate the NDVI anomaly, the mean NDVI (NDVI_i mean) from September to January (the growing season) of each year was initially determined using the following formula.

$$\mathrm{NDVI\ mean}i = (\mathrm{NDVI}1 + \mathrm{NDVI}2 + \cdots \mathrm{NDVI}n)/n \quad \text{(eq.2)}$$

Where NDVI meani represents mean NDVI value of the growing season of “i”

35

year. NDVI1 is the first 5 to 10 days, NDVI2 is the second 5 to 10 days and to NDVIn which is the last 5 to 10 days NDVI composite during the growing season of “i” year.

Once the NDVI mean for each growing season over the 5-year period was calcultaed, the overall mean of these NDVI values were determined using the following formula.

$$\text{Over All NDVI} = \sum_{i=1}^{n}(\text{NDVImeani})/n \quad \text{(eq.3)}$$

Where n represents the number of years which is equal to 5 years. Then, the seasonal NDVI anomaly was derived using the following formula.

$$\text{NDVIanomaly i} = \frac{\text{NDVImeani} - \text{OANDVI}}{\text{OANDVI}} * 100$$

(eq.4)

Where NDVI anomaly i is the NDVI anomaly for the growing season during “i” year.

Vegetation condition index

Kogan (1995) introduced the Vegetation Condition Index (VCI), which is based on the relative change in NDVI compared to the minimum historical NDVI value, NDVImin (x, y). It is defined as follows:

$$\text{Max NDVI} = \text{Max}(\text{NDVI1}, \text{NDVI2}, \text{NDVI3} \ldots \text{NDVIn}) \quad \text{(eq.5)}$$

$$\text{Min NDVI} = \text{Min}(\text{NDVI1}, \text{NDVI2}, \text{NDVI3} \ldots \text{NDVIn}) \quad \text{(eq.6)}$$

Where Max NDVI is maximum NDVI from the time series data, while Min NDVI is minimum NDVI from the time series data. This was done by cell statistics tool of ArcGIS software.

$$\text{VCI} = \text{NDVI}(x, y) - \frac{\text{minNDVI}(x,y)}{\text{maxNDVI}(x,y) - \text{NDVImin}(x,y)} * 100 \quad \text{(eq.7)}$$

Where VCI is Vegetation Condition Index, min NDVI and max NDVI is minimum and maximum NDVI value in the time series data respectively. Hence, in the current research work, the calculation of VCI was done by raster calculator tool of ArcGIS software. Fig. 2 indicates the framework of the study.

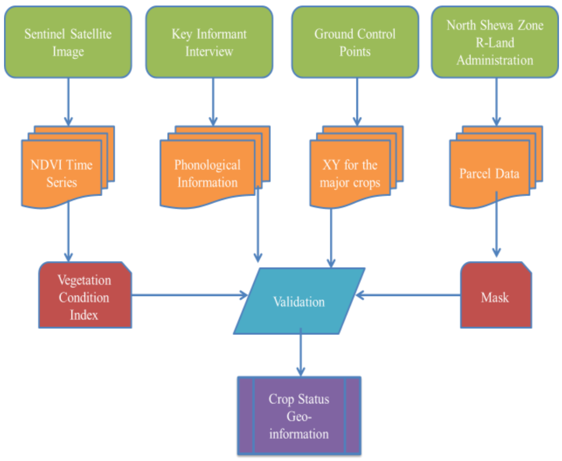

Figure 2. Framework of the study

Results and Discussion

Phenology of major crops

The changes in the timing of regional vegetation growth stages indicate how ecosystems respond to climate change. The timing of these cycles is a useful measure for understanding the interactions between vegetation and climate, as well as their impact on carbon cycling (White et al., 2009). The phenology of crops offers crucial insights for planning irrigation, managing fertilizers, understanding seasonal carbon dioxide (CO2) exchange in ecosystems, and estimating biomass productivity (You et al., 2013). Therefore, promptly and accurately identifying crop phenology is essential not only for studying climate variability but also for the efficient and scientific utilization of farmland. Typically, agricultural crops exhibit a characteristic NDVI pattern: a decline at the start of the growing season (indicating tillage), high values during the peak growth phase (indicating full bloom), and another decline at the end of the season (indicating harvest) (Kanjir et al., 2018).

The annual vegetation phenology cycle, as observed through remote sensing, is marked by four significant transition dates that outline the main phenological stages of vegetation dynamics yearly. These dates are: (1) green-up, when photosynthetic activity begins; (2) maturity, when the green leaf area of plants is at its peak; (3) senescence, when photosynthetic activity and green leaf area start to decline rapidly; and (4) dormancy, when physiological activity is nearly zero (Zhang et al. 2003). Crop phenology studies require frequent observation of the target. In this study, Sentinel satellite image with five days of temporal resolutions were used. Due to thick cloud cover in the early growing period, only cloud free images of July, August and September were used. Based on the observed crop pattern trends in the study area, phenology detection was conducted for the four main crops; Teff, Onion, Wheat, and Sorghum. Our analysis indicates that July 12 marked the start of the growing season for all crops, primarily associated with seedling emergence. The high NDVI value for Teff was detected on August 26 while October 5 was the date of highest NDVI value for wheat. Highest NDVI values for Onion and Sorghum were observed on September 15. These peaks in the phonology graph indicate the dates of maximum greening stage (Fig.3).

Following the peak greening stage, a gradual decline in NDVI values for all crops is observed. November 9 was the date of Senescence for Teff and Wheat, whereas November 14 was for Sorghum. The date of senescence for onion was October 25. The end of growing season (harvesting period) for Onion was around November 9, for Wheat it was November 14. November 19 marked the harvesting time for Teff and Sorghum (Table 2 & Fig.4).

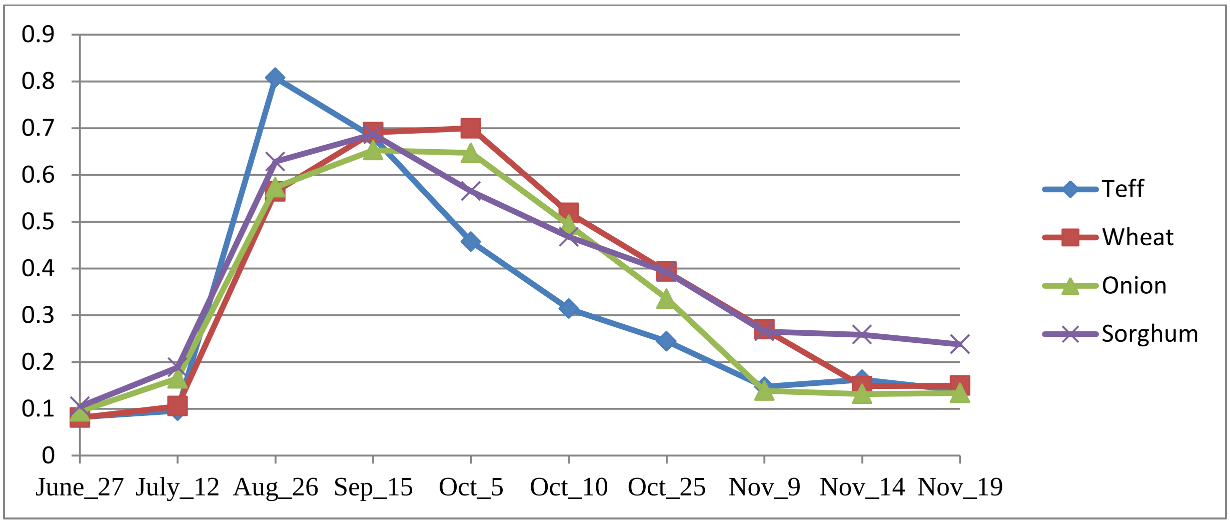

Figure 3. Phenology graph

Table 2: The phenology of major crops

SN	Crop Name	Sowing	Emergence	Max greening	Senescence	Harvesting	Remark
1	Teff	July1-30	Aug 1-30	Sep 1-30	Sep 23-30	Oct 1-Dece 15	
2	Onion	June 23-July 7	July 23- 31		Sep 23-30	Sep23- Octo 15	
3	Wheat	July1-30	Aug 1-30	Sep 1-30	Sep 23-30	Oct 23-Nov 15	From agricu. office gricultural Office
4	Sorghum		July 1-30	Sep 1-30	15-Oct	Nov1- Dec 31	
5	Teff	27-Jun	12-Jul	26-Aug	9-Nov	19-Nov	
6	Onion	27-Jun	12-Jul	15-sep	25-Oct	9-Nov	NDVI Result
7	Wheat	27-Jun	12-Jul	5-Oct	9-Nov	14-Nov	
8	Sorghum	27-Jun	12-Jul	15-Sep	14-Nov	19-Nov	

Although statistically linking the phenology is not particularly significant, Table 2 demonstrates that the phenology of major crops derived from NDVI is related to the reference information from the agricultural office.

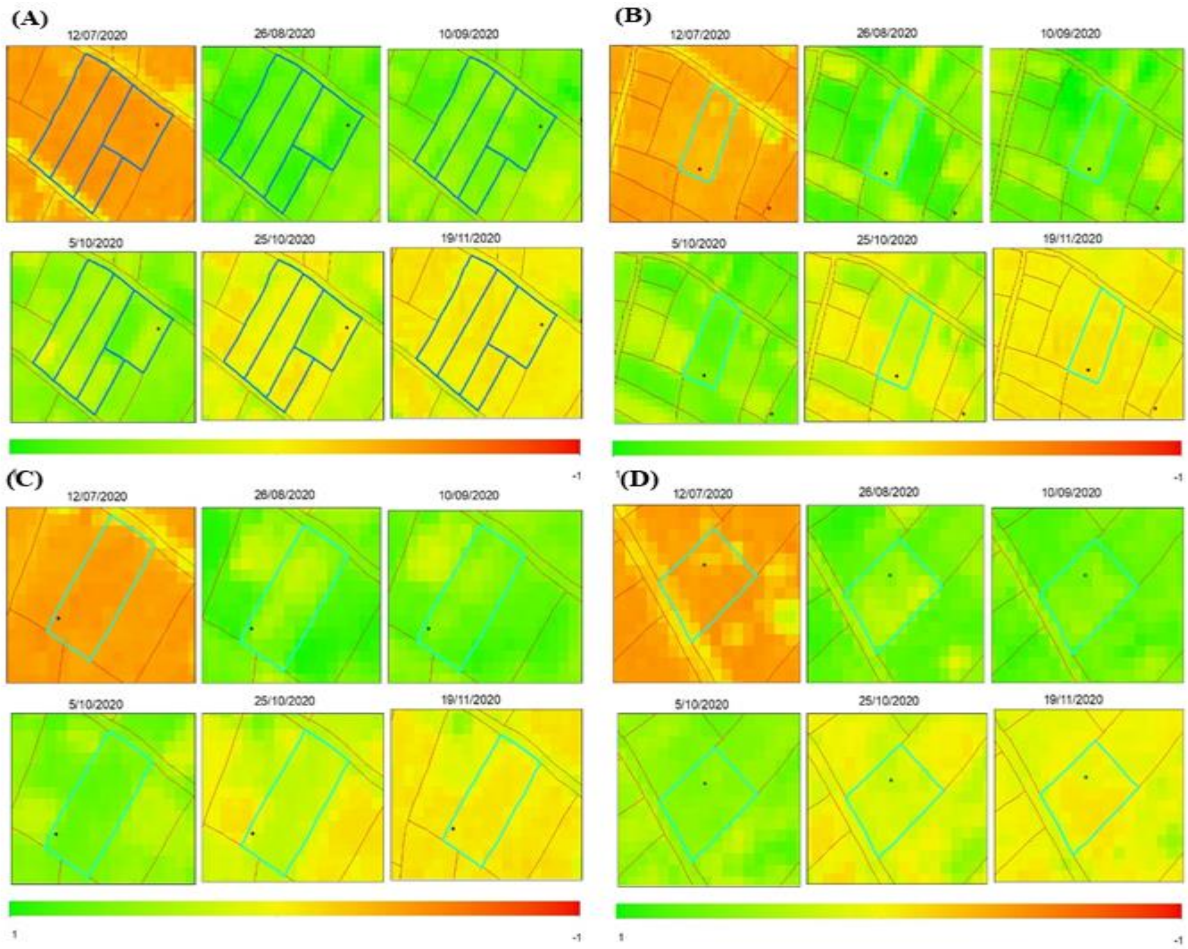

Figure 4: Phenology maps of (A) Teff, (B) Onion, (C) Wheat and (D) Sorghum

Crop type mapping

In the study area, crop land data was typically collected and shared through expert observations and farmer interviews. Nevertheless, these methods are time-consuming, labor-intensive, less efficient, and expensive in providing parcel-level information to stakeholders. In contrast, crop maps derived from satellite images offer a more efficient alternative for accurate crop data collection, documentation, and communication (Thiruvengadachari and Sakthiyadivel, 1997; Lobell et al., 2003; Thenkabail et al., 2010). Accordingly, using Sentinel satellite imagery, the study area was classified and mapped into various land use and land cover types, with a focus on identifying major crop type. To achieve this, ground control points were gathered from the field to classify and validate the created crop map.

39

Table 3: Crop covers statistics

SN	Name	Area	Percent
1	Teff	7934.95	67
2	Onion	1554.73	13
3	Wheat	1222.18	10
4	Sorghum	1189.70	10
5	Total	11901.56	100

As it is shown in Table 3, approximately 67% of the cultivated land is covered with Teff, reflecting its widespread popularity in the Menjar Shenkora district. Onions account for about 13% of the crop distribution, while the remaining 20% is equally divided between wheat and sorghum. Figure 5 also illustrated how each crop was distributed throughout the study area.

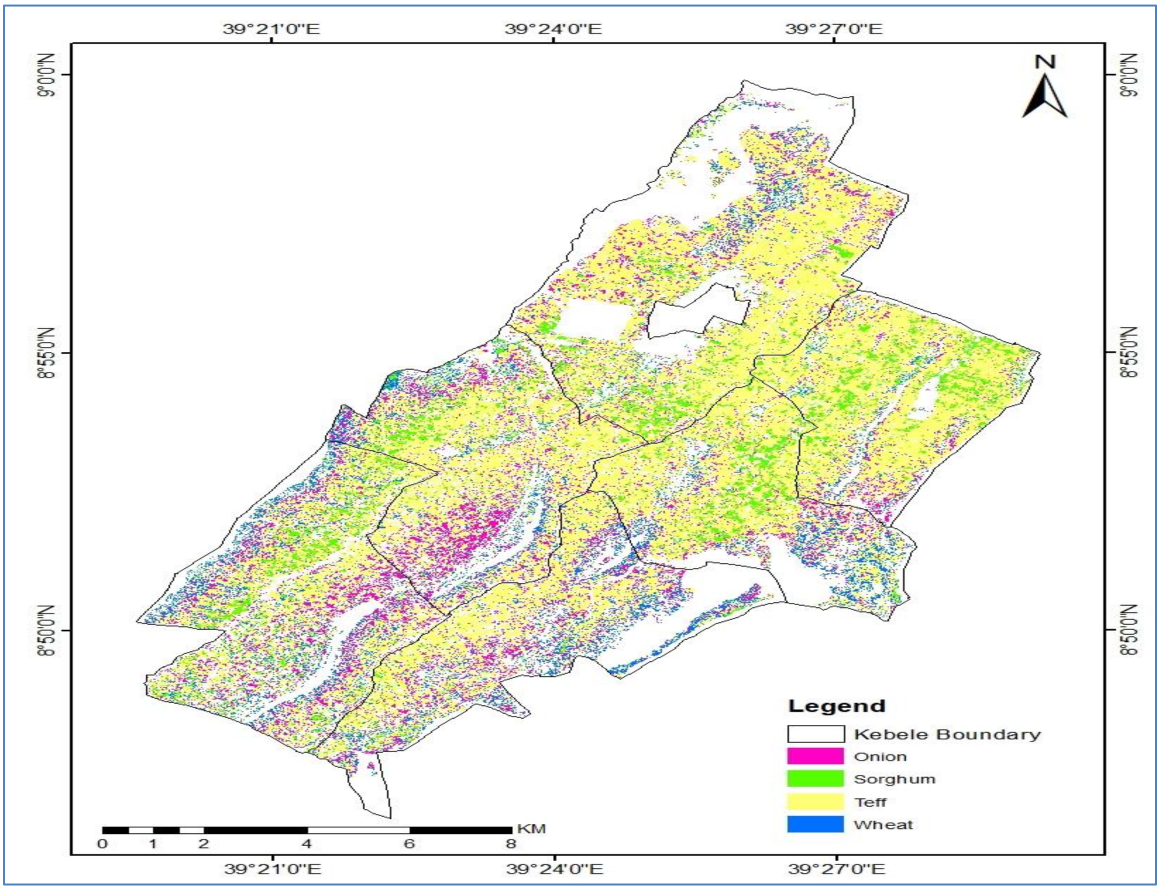

Figure 5. Crop map of the study area

The crop type map achieved an overall classification accuracy of 79.26% and a kappa value of 0.737 (Table 4). Consequently, our classification results have a deviation of 20.74%. Crop area statistics gathered by various stakeholders, including non-governmental organizations and agricultural offices, typically exhibit deviations of up to 30% and do not accurately reflect the actual cultivated area (Van Genderen et al. 1978; Stehman et al. 2003; Gallego 2004; Biggs et al. 2006).

Table 4: Accuracy report

	Crop Types	Reference						
		Teff	Onion	Wheat	Sorghum	Total	User Accuracy	Kappa
Classified	Teff	18.00	1.00	1.00	0.00	20.00	90.00	0.737
	Onion	1.00	14.00	3.00	2.00	20.00	70.00	
	Wheat	3.00	1.00	16.00	2.00	22.00	72.73	
	Sorghum	0.00	1.00	2.00	17.00	20.00	85.00	
	Total	22.00	17.00	22.00	21.00	82.00		
	Producer Accuracy	81.82	82.35	72.73	80.95	OA=79.26		

Crop status monitoring

Information on crop status is essential for decision-making in both private and public sectors involved in food self-sufficiency, agricultural policy and production. Crop conditions can change rapidly due to factors like soil moisture, fertilization, temperature, or disease etc. As a result, it is crucial to frequently observe crops with comprehensive geospatial coverage and adequate detail throughout the growing season to effectively monitor their conditions (Yang et al., 2011).

Chappelle et al., (1992) reported that due to strong absorption by photosynthetic and accessary pigments, green plant leaves show low reflectance and transmittance in the visible electromagnetic spectrum (400 to 700 nm). Conversely, because of minimal absorption by subcellular particles or pigments and significant scattering at mesophyll cell wall interfaces, they exhibit high reflectance and transmittance in the near-infrared spectrum (700 to 1300 nm) (Gausman, 1974; Slaton et al., 2001). This distinct difference in reflectance between visible and NIR wavelengths facilitates many remote sensing techniques for monitoring and managing crops and natural vegetation.

In this study, we used VCI to generate and quantify crop status information. As it is clearly shown in Table 5, anomaly information for the parcels is classified in to five classes as extreme anomaly, severe anomaly, moderate anomaly, normal condition and better than average (Luisa, 2017). According to October 1-10 anomaly result, about 78.56% of the study area is in a better than average anomaly class. This percentage value is 5%, 4.06, 2.09% and 10.29% for normal condition, moderate anomaly, severe anomaly and extreme anomaly respectively.

Table 5: crop status information

Name	Area (Oct 1-10)	%	Area (Oct 20-30)	%	Area (Nov 1-10)	%	Area (Nov 10_20)	%
E Anomaly	1634.69	10.29	2376.70	14.96	2145.98	13.51	549.50	3.46
S Anomaly	332.67	2.09	990.92	6.24	1741.82	10.96	1146.23	7.21
M Anomaly	644.71	4.06	1726.28	10.86	2681.61	16.88	1161.98	7.31
N Condition	794.78	5.00	1782.80	11.22	2362.60	14.87	1463.74	9.21
B Than AVG	12481.94	78.56	9012.09	56.72	6956.78	43.78	11567.34	72.80
Total	15888.79	100.00	15888.79	100.00	15888.79	100.00	15888.79	100.00

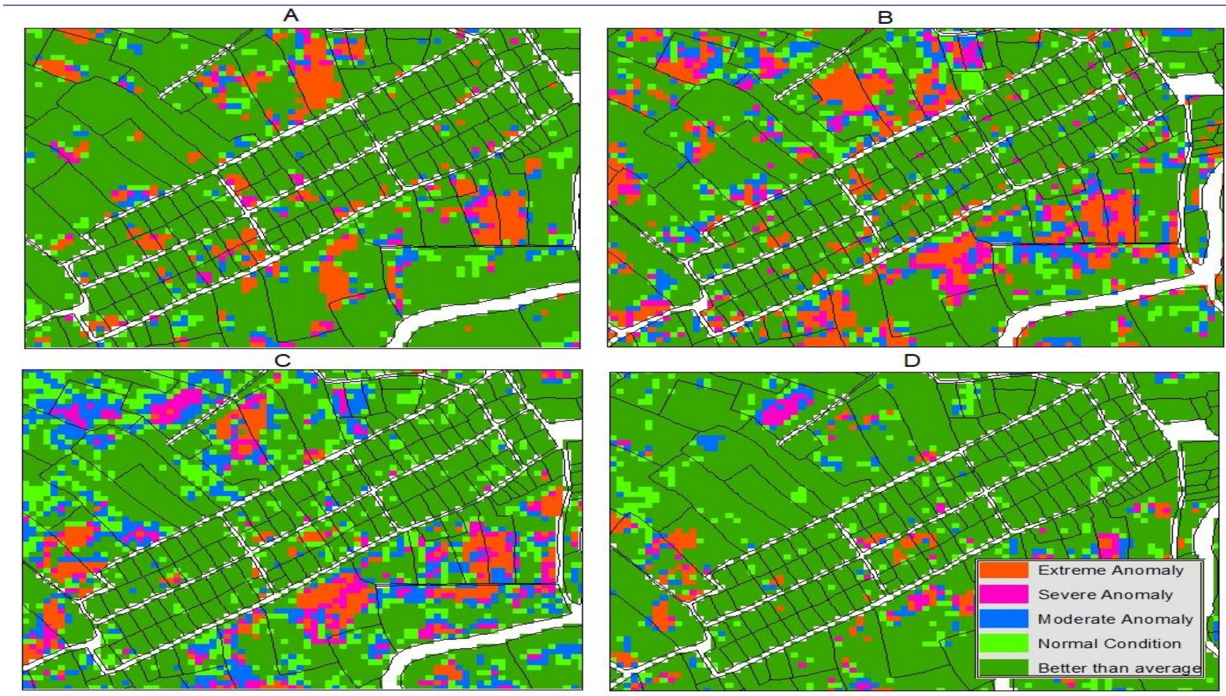

Figure 6: Crop status map

In the second date of anomaly analysis, the share of better than average anomaly class decreased significantly to 56.72%. Conversely to this, the percentage of extreme anomaly and severe anomaly increased to 14.96% and 6.24%, respectively. In this measurement date, the percentage share for extreme anomaly and severe anomaly is about 13.51% and 10.96%, respectively. In the last measurement date the share of better than average increased to 72.80 %. In contrary to this, the share of extreme anomaly and severe anomaly decreased to 3.46% and 7.21% correspondingly (Table 5). In his study, crop condition information is prepared and mapped for each parcel for the selected kebeles of Menjar Shenkora district (Fig. 6).

Conclusions

The main objective of this study was to gather geo-information on crop health. To achieve this, NDVI time series data was generated using Sentinel satellite images obtained from the official Sentinel Hub website (sentinel-hub.com). Crop health monitoring is one of the important items for tracking the general health status of any crop. In this regard remote sensing and GIS plays a crucial role for monitoring crop health, providing current information that traditional methods like field surveys and sampling questionnaires struggle to obtain. Effective cropland mapping techniques are essential for regular crop monitoring. In the study the effectiveness of geospatial methods and Optical data was tested and they are proved to be effective with some limitations. The output of the current research gives information about the onset, greening, maturity and senescence dates for Teff, Wheat, Onion and Sorghum. Based on our analysis, the growing season for all crops begins on July 12, coinciding with the onset of photosynthetic activity. The highest NDVI value for Teff is observed on August 26, while for wheat, it peaks on October 5. For Onion and Sorghum, the highest NDVI values are recorded on September 15, corresponding to the maturity stage when the plant's green leaf area is at its maximum. All other stages are similarly captured by NDVI and these findings align with the field data collected from the relevant office. A crop type map for the major crops in the selected kebeles of Menjar Shenkora district shows that 67% of the cultivated land is covered by Teff, the most popular crop in the area. Onion, Wheat, and Sorghum account for approximately 13% and 10% of the land, respectively. Additionally, a crop health status map was created, classifying conditions as Extreme anomaly, Severe Anomaly, Moderate anomaly, Normal condition, and better than average at four different time periods.

Finally, in comparison to traditional crop monitoring methods, remote sensing offers a more continuous, accurate, and effective way to monitor crop health. Therefore, we recommend stakeholders adopt this approach. Mapping crop types requires extensive ground control points for various crops, so collecting detailed field data across multiple parcels can enhance crop type mapping. Thick cloud cover posed a significant challenge for analyzing crop phenology and health status, making

43

reliance solely on optical bands from Sentinel satellite imagery problematic. Hence, we advise other researchers to utilize both optical and Synthetic Aperture Radar (SAR) data.

Acknowledgments The authors would like to express their gratitude to Debre Berhan University for the financial support, to the experts, and farmers from the Minjar Shenkora district agricultural office for supplying the necessary data. Besides, the authors appreciate the anonymous reviewer for his/her insightful comments and suggestion which in return improved our manuscript.

Contributions by the Authors

AD, AB, and EL collaboratively designed the study, gathered, analyzed, and interpreted the data, wrote and edited the manuscript.

Disclosure The authors affirm that the manuscript's content is original and has neither been published nor submitted for publication elsewhere.

Conflicts of Interest The authors declare no conflicts of interest.

Funding This study was funded by Debre Berhan University.

References

Anyamba, A., Tucker, C.J., (2012). Historical perspective of AVHRR NDVI and vegetation drought monitoring. In: Remote Sensing of Drought: Innovative Monit Approaches, pp. 23. https://doi.org/10.1201/b11863-4/r10.1201/b11863-4.

Atzberger, C. (2013). Advances in remote sensing of agriculture: Context description, existing operational monitoring systems and major information needs. Remote sensing, 5(2), 949-981.

Biggs T.W, Thenkabail PS, Gumma MK, Scott CA, Parthasaradhi GR, Turral HN. (2006). Irrigated area mapping in heterogeneous landscapes with Modis time series, ground truth and census data, Krishna basin, India. Int J Remote Sens. 27(19):4245–4266. Available from: http://www.informaworld.com/10.1080/01431160600851801.

Bouchet, A.S., Laperche, A., Bissuel-Belaygue, C., Snowdon, R., Nesi, N. and Stahl, A., (2016). Nitrogen use efficiency in rapeseed. A review, Agron. Sustain. Dev. 36(2), 38 (2016).

Bradley, B. A., Jacob, R. W., Hermance, J. F., & Mustard, J. F. (2007). A curve fitting procedure to derive inter-annual phenologies from time series of noisy satellite NDVI data. Remote Sensing of Environment, 106, 137–145. doi:10.1016/j.rse.2006.08.002.

Chappelle, E.W., M.S. Kim, and J.E. (1992). Ratio analysis of reflectance spectra (RARS) – An algorithm for the remote estimation of the concentrations of chlorophyll-a, chlorophyll-b, and carotenoids in soybean leaves, Remote Sensing of Environment, 39(3):239–247.

Central Statistical Agency (CSA) (2013). National Labor Force Survey Report, Addis Ababa, Ethiopia

Defourny, P., Bontemps, S., Bellemans, N., Cara, C., Dedieu, G., Guzzonato, E., ... & Savinaud, M. (2019). Near real-time agriculture monitoring at national scale at parcel resolution: Performance assessment of the Sen2-Agri automated system in various cropping systems around the world. Remote sensing of environment, 221, 551-568.

Diacono, M., Rubino, P. and Montemurro, F., (2013). Precision nitrogen management of wheat. A review, Agron. Sustain. Dev. 33(1), 219–241 (2013).

Duchemin, B., Fieuzal, R., Rivera, M. A., Ezzahar, J., Jarlan, L., Rodriguez, J. C., Hagolle, O. and Watts, C., (2015). Impact of Sowing Date on Yield and Water Use Efficiency of Wheat Analyzed through Spatial Modeling and FORMOSAT-2 Images, Remote Sens. 7(5), 5951–5979 (2015).

Gallego F.J. (2004). Remote sensing and land cover area estimation. Int J Remote Sens. 25(15):3019–3047.

Gascon, F., Bouzinac, C., Thépaut, O., Jung, M., Francesconi, B., Louis, J., Lonjou, V., Et al., (2017). Copernicus Sentinel-2A Calibration and Products Validation Status. Remote Sens. 2017, 9(6), 584; https://doi.org/10.3390/rs9060584

Gausman, H.W., and W.G. Hart, (1974). Reflectance of sooty mold fungus on citrus leaves over 2.5 to 40-micrometer wavelength interval, Journal of Economic Entomology, 67(4):479–480.

Getachew B., Hill S.,Tsegaye T. and Solomon A. (2011). Using Satellite Images for Drought Monitoring: A Knowledge Discovery Approach. Journal of Strategic Innovation and Sustainability Vol. 7(1).

Hatfield, P. L. and Pinter, P. J., (2016). Remote sensing for crop protection. Crop Prot. 12(6), 403–413 (1993).

Vreugdenhil, M., Pfeil, I., Riffler, M., Kolitzus, D., Dorninger, P. and Wagner, W., (2018). Monitoring vegetation dynamics using Sentinel-1 and Sentinel-2. Presented at EGU General Assembly Conference Abstracts, 1 April 2018, 12559.

Kogan, F. N., (1995). Application of Vegetation Index and Brightness Temperature for Drought Detection", Advanced Space Research, Vol. 15, No. 11, pp. (11)91-100, 1995.

Lobell DB, Asner GP, Ortiz-Monasterio JI, Benning TL. 2003. Remote sensing of regional crop production in the Yaqui valley, Mexico: Estimates and uncertainties. Agric Ecosyst Environ. 94(2):205–220. Available from: http://www.sciencedirect.com/science/article/B6T3Y-45CW274-1/2/53a983e89193412b917f97e05211c703.

Luisa F. Amalo R. H, and Sayidah S. (2018). Analysis of Agricultural Drought in East Java Using Vegetation Health Index. AGRIVITA Journal of Agricultural Science. 2018. 40(1): 63-73.

Maas, S. J., (1988). Use of remotely-sensed information in agricultural crop growth models. Ecol. Model. 41(3), 247– 268 (1988).

Matteo G. Z, Muhammad U. Altaf, B.A., Rasmus H., Trenton E. F., Yang L., Justin S., Ibrahim H. , Matthew F.M (2022). Early season prediction of within-field crop yield variability by assimilating CubeSat data into a crop model. Agricultural and Forest Meteorology, Volume 313, 2022, 108736.

National Bank of Ethiopia. (2013). Annual Report, Addis Ababa, Ethiopia.

Prathumchai, K. Honda, et al. (2001). Drought Risk Evaluation using Remote Sensing and GIS: A case study in Lop Buri Province. 22nd Asian Conference on Remote Sensing.

Rojas, M. R., & Gilbertson, R. L. (2008). Emerging plant viruses: a diversity of mechanisms and opportunities. In Plant virus evolution (pp. 27-51). Springer, Berlin, Heidelberg.

Slaton, M.R., E.R. Hunt, and W.K. Smith, (2001). Estimating near infrared leaf reflectance from leaf structural characteristics,

Stehman S.V, Wickham J, Smith J, Yang L. (2003). Thematic accuracy of the 1992 national land-cover data for the eastern united states: Statistical methodology and regional results. Remote Sens Environ. 86 (4): 500–516.

Thenkabail P, Hanjra M, Dheeravath V, Gumma M. (2010). A holistic view of global croplands and their water use for ensuring global food security in the 21st century through advanced remote sensing and non-remote sensing approaches. Remote Sens. 2(1):211–261.

Thiruvengadachari S, Sakthivadivel R. (1997). Satellite remote sensing for assessment of irrigation system performance: A case study in India. Research report 9. Colombo, Sri Lanka: International irrigation management institute.

Tucker, C. J. (1979). Red and photographic infrared linear combinations for monitoring vegetation. *Remote sensing of Environment*, *8*(2), 127-150.

Van Genderen J, Lock B, Vass P. (1978). Remote sensing: Statistical testing of thematic map accuracy. Remote Sens Environ. 7(1):3–14.

Verbesselt, J., Zeileis, A., & Herold, M. (2012). Near real-time disturbance detection using satellite image time series. Remote Sensing of Environment, 123, 98-108.

White, M.A., de Beurs, K.M., Didan, K., Inouye, D.W., Richardson, A.D., Jensen, O.P., et al., (2009). Intercomparison, interpretation, and assessment of spring phenology in North America estimated1071 from remote sensing for 1982-2006. Global Change Biol. 15, 2335-2359.1072. https://doi.org/10.1111/j.1365-2486.2009.01910.x

Wubne, M. (1991). Agriculture (and subsections). A Country Study: Ethiopia (Thomas P. Ofcansky and

LaVerle Berry, eds.) Library of Congress Federal Research Division (1991).

You X., Jihua M., Miao Z. and Taifeng D. (2013). Remote Sensing Based Detection of Crop Phenology for Agricultural Zones in China Using a New Threshold Method. Remote Sens. 2013, 5, 3190-3211; doi:10.3390/rs5073190.

Yang, Z., Di, L., Yu, G., & Chen, Z. (2011). Vegetation condition indices for crop vegetation condition monitoring. In 2011 IEEE International Geoscience and Remote Sensing Symposium (pp. 3534-3537). IEEE.

Zhang, D., Fang, S., She, B., Zhang, H., Jin, N., Xia, H., ... & Ding, Y. (2019). Winter Wheat Mapping Based on Sentinel-2 Data in Heterogeneous Planting Conditions. Remote Sensing, 11(22), 2647.

Zhang, X., Friedl, M. A., Schaaf, C. B., Strahler, A. H., Hodges, J. C. F., Gao, F., & Huete, A. (2003). Monitoring vegetation phenology using MODIS. Remote Sensing of Environment, 84, 471–475. doi:10.1016/ S0034-4257(02)00135-9.